Dear Author,

Please, note that changes made to the HTML content will be added to the article before publication, but are not reflected in this PDF.

Note also that this file should not be used for submitting corrections.

AUTHOR QUERY FORM

Dear Author,

Please check your proof carefully and mark all corrections at the appropriate place in the proof (e.g., by using on-screen annotation in the PDF file) or compile them in a separate list. Note: if you opt to annotate the file with software other than Adobe Reader then please also highlight the appropriate place in the PDF file. To ensure fast publication of your paper please return your corrections within 48 hours.

For correction or revision of any artwork, please consult http://www.elsevier.com/artworkinstructions.

Any queries or remarks that have arisen during the processing of your manuscript are listed below and highlighted by flags in the proof. Click on the Q link to go to the location in the proof.

Your article is registered as a regular item and is being processed for inclusion in a regular issue of the journal. If this is NOT correct and your article belongs to a Special Issue/Collection please contact v.raman@elsevier.com immediately prior to returning your corrections.

Location in article	Query / Remark: **click on the Q link to go** Please insert your reply or correction at the corresponding line in the proof
Q1	Please confirm that given names and surnames have been identified correctly and are presented in the desired order.
Q2	Highlights should only consist of 85 characters per bullet point, including spaces. The highlights provided are too long; please edit them to meet the requirement.
Q3	The reference given here is cited in the text but is missing from the reference list – please make the list complete or remove the reference from the text: "WHO Guidelines, 2010".
Q4	Please provide the Grant number for the Grant sponsor "Area Science Park of Trieste".
Q5	Please check whether the Ref. [17] is okay as set.
Q6	Please check whether the year in Ref. [22] is okay as amended.

Thank you for your assistance.

Please check this box or indicate your approval
if you have no corrections to make to the PDF file

Highlights

Novel image processing approach to detect malaria

Optics Communications ∎ (∎∎∎∎) PP. 3–5

Q1 David Mas, Belen Ferrer, Dan Cojoc, Sara Finaurini, Vicente Mico, Javier Garcia, Zeev Zalevsky

- Novel image processing algorithm providing good preliminary capabilities for in vitro detection of malaria.
- The algorithm is based upon analysis of the temporal variation of each pixel.
- Q2 Changes in dark pixels mean that inter cellular activity happened, indicating the presence of the malaria parasite.
- Preliminary experimental results involving analysis of red blood cells validated the potential benefit of the proposed approach.

Novel image processing approach to detect malaria

David Mas [a], Belen Ferrer [b], Dan Cojoc [c], Sara Finaurini [c], Vicente Mico [d], Javier Garcia [d], Zeev Zalevsky [e],*

[a] University Institute of Physics Applied to Sciences and Technologies, University of Alicante, Alicante 03080, Spain
[b] Department of Civil Engineering, University of Alicante, Alicante 03080, Spain
[c] CNR-IOM Institute of Materials, Area Science Park—Basovizza, S.S. 14 km 163.5, Trieste 34149, Italy
[d] Departamento de Óptica, Universitat de València, c/Dr. Moliner, 50, 46100 Burjassot, Spain
[e] Faculty of Engineering, Bar Ilan University, Ramat Gan 5290002, Israel

ARTICLE INFO

ABSTRACT

In this paper we present a novel image processing algorithm providing good preliminary capabilities for in vitro detection of malaria. The proposed concept is based upon analysis of the temporal variation of each pixel. Changes in dark pixels mean that inter cellular activity happened, indicating the presence of the malaria parasite inside the cell. Preliminary experimental results involving analysis of red blood cells being either healthy or infected with malaria parasites, validated the potential benefit of the proposed numerical approach.

© 2015 Published by Elsevier B.V.

1. Introduction

Malaria is a life-threatening infectious disease with global impact: more than 200 million cases every year and ongoing malaria transmission in about 100 countries [1]. The statistics that the World Health Organization (WHO) has revealed on malaria is very large. Below there are some numbers that are relevant to illustrate the earnest of this disease:

(i) about 3.4 billion people are at risk of malaria
(ii) more than one malaria case occurs per 1000 population in high risk areas
(iii) about 627,000 malaria deaths in 2012 (of which 90% in sub-Saharan Africa)
(iv) about 482,000 children killed by malaria in 2012 (i.e. two children almost every minute).

Even if malaria is an entirely preventable and treatable mosquito-borne illness in western countries, in developing countries this situation is possible due to an inadequate funding to struggle malaria. Some progress has been however done in the last decade, allowing reducing malaria incidence rates by 25% globally, and by 31% in the WHO African Region. These interventions saved an estimated 3.3 million lives of which 90% are in the under-five age group in sub-Saharan Africa.

This global issue has stimulated the interest in developing new diagnostic strategies since malaria is often under-diagnosed and over-cured [2]. Prompt and accurate diagnosis is essential to prevent morbidity and mortality avoiding the risk of increasing drug resistance due to unspecific therapy. Up to date, the gold standard in malaria diagnosis remains the examination of stained blood films by optical microscopy [3]. Unfortunately, poor laboratory conditions in endemic countries result in high rate of false diagnostic results, leading to inappropriate therapy and to malaria overspread. Accurate diagnosis takes considerable time and only the experience of a well trained microscopist can reduce errors [3]. Especially for the lethal *Plasmodium falciparum (P.f),* the prompt life saving treatment requires high sensitive diagnosis and rapid access to the test results. Therefore, a diagnostic tool for malaria in endemic countries must be: rapid, accurate, simple to use, low cost and easily interpretable (WHO Guidelines, 2010).

The way in which the parasite development induces changes of the host red blood cell (RBC) membrane and cytoskeleton is very complex, since more than 100 proteins of the host RBC can suffer modifications with important impact on the properties of the infected RBC and on malaria pathogenesis [4]. Progressive stiffness of the cell membrane is associated with the parasite growth [5,6]. The biomechanical properties of the uninfected RBCs present in parasitized blood are also altered in vitro and in vivo, but the

mechanism and the causes are still unclear [7–9]. Several techniques have been recently proposed to measure biomechanical changes of the cells. These include microfluidics, photoacoustic and optical techniques. Microfluidics is based on recent progress in fabrication of microchannels with properties similar to that of the blood vessels [10,11]. Exploiting hemodynamic effects as the Fahraeus effect or margination, plasma separation and white blood cell enrichment have been demonstrated [12,13]. The margination effect, based on the deformability of RBCs, has also been employed to segregate infected RBCs from non infected cells in malaria [14]. Interestingly, the separation effect is maximum in 40% hematocrit, allowing processing a large number of cells/unit of time. However, this technique is limited to 90% recovery for late stage (thropozoite) infected RBCs and 75% recovery for early stage (ring) infected RBCs. The performance of the approach of [14] in terms of accuracy, is still far from that of Giemsa method but it can be used as a preliminary step to increase the concentration of infected cells in a given blood sample [3]. A microfabricated deformability-based flow cytometer with micro-pillars having suitable size, shape and gap between them, has also been proposed for the separation of the infected RBCs [15]. Photoacoustic microscopy and flow cytometry has been also involved to infer the size, shape and orientation of RBCs or real-time detection of circulating cancer cells [16–18]. Optical techniques are mainly based on diffraction and interferometry microscopy approaches. Diffraction phase microscopy [19] has thus been proposed for an accurate characterization of the dynamics of the cell membrane. This allows measuring the cell membrane stiffness, and distinguishing between different elements of the cell [20]. Speckle sensing microscopy [21] and shearing interferometry [22] schemes have been proposed for fast and automated detection of malaria. Moreover, multimodal imaging in microscopy provided by the combination of different techniques is a valuable tool for quantifying information about cell dynamics and evolutions at nanoscale range by cross-checking information between them [23–27]. By multimodal imaging we refer to using a single optical source and single camera to image amplitude, phase, and fluorescence features of a biological specimen. Additional recent progress on RBC morphology characterization can be found in [28–30].

In this paper we present a novel image processing approach based upon localizing the movement of the cells and inspecting whether this movement has some type of spatial dependence. The software used is freely available at [31] and is available for the most used platforms. Additionally the process is simple and fast since it does not require high computational resources. In our processing we take the temporal variation of each pixel, a voxel, and consider it as an independent set. The temporal average of each voxel provides the average brightness of a pixel and gives an indication of movement of sub cellular organisms. The obtained statistics show that the proposed algorithm may have applicability for real time fast and automatic process of malaria detection.

Thus, instead of analyzing the movement pattern of the cell membrane that is flickering due to the thermal vibration and compare it with the data obtained from healthy cell as done in [21], in the current paper we decided to localize the movement and see if there was a spatial dependence. Usually video sequences are considered as series of consecutive frames. Here we consider them as a three-dimensional hyper structure. Therefore, the temporal variation of each pixel is considered as an independent set. This structure is known as "voxel" from the words "volume pixel". Each of these structures carries information about luminance time-variation of a single pixel. Taking the temporal average of each voxel provides the average brightness of a pixel: if this is high, it means that an object was there, and if it is dark, there was no object at all. Temporal standard deviation informs about the activity of this pixel. A high standard deviation means that the value of the pixel changes along the sequence while low temporal standard deviation reports about low activity. In order to make a fair comparison, the value of the standard deviation (STD) is renormalized by the mean value, so activity of the pixel is referred to its mean state. This way we reduce the whole sequence to a single image where each pixel is the:

$$s_n = \frac{s_0 - \text{STD}(x, y)}{s_0 - \text{mean}(x, y)} \tag{1}$$

where s_n is the new pixel value and s_0 is the pixel's original value (i.e. Eq. (1) presents a computation resulting in new pixels value and therefore in a new image obtained after applying the computation of Eq. (1) on the original image captured by the camera). Changes of ± 10 in the pixels value in a bright area can be due to changes in the position of the cell, but in a dark area could mean some real activity.

The detection idea in the above technique speculates on the presence, development and movement of the parasite inside the infected RBC. Malaria infection starts when the parasite breaks the cellular erythrocytic membrane and invades a new RBC. At this stage the parasite is called ring. Then, it grows by destroying hemoglobin becoming a trophozoite, which finally undergoes to cellular division, namely schizont. These are forms that change the dynamics of the cell movement with respect to an uninfected cell. The voxel based method we are proposing reduces the temporal stack of images in the video sequence into a single image, which contains enough information to classify the cell as either being infected or as an uninfected cell.

2. Materials and methods

2.1. Sample preparation

Donor blood was kindly provided by the Blood Bank Service of Azienda Ospedaliero-Universitaria Ospedali Riuniti di Trieste (nonprofit organization for blood donation). Citrate-anticoagulated blood was obtained from healthy A-positive donors after informed consent. Aliquots of blood were centrifuged at 2300 rpm for 13 min to remove the buffy coat and the erythrocyte pellet was washed three times with 5 mM phosphate-buffered saline (PBS). P.f (W2 strain) culture was carried out according to Trager and Jensen [32] and maintained at 5% hematocrit (human type A-positive red blood cells) in RPMI 1640 medium with the addition of 1% AlbuMax, 0.01% hypoxantine, 20 mM Hepes, and 2 mM glutamine. Synchronous cultures with parasitaemia of 4%–5% were diluted to 0.01% final hematocrit, aliquoted into a petri dish and incubated at 37 °C. P.f cultures in a defined stage (rings and throphozoits) were obtained using the synchronized protocol. Briefly, parasite cultures were suspended in 5% D-sorbitol and subsequently were reintroduced into new freshly prepared cultures. In fact, after sorbitol treatment, cultures consisted of rings (early stage). After 24 and 72 h of culture, a high percentage of rings and trophozoite were respectively present. Both the parasitaemia and P.f culture stage were checked by Giemsa staining of a blood smear, before the optical experiments.

2.2. Optical microscopy, video acquisition and image processing

The petri dish with the RBC samples at different stages was placed on the stage of an inverted microscope and imaged in bright field under white illumination (Halogen lamp, 100 W) through a 100X objective (PL APO 100x/1 water, Olympus) onto the sensor of a CMOS camera (Fastec Hispec-4, from Gold Elettronica, Chiavari, Italy). The camera had 1696 × 1710 pixels while

the magnification of the microscope was such that in each image the inspected cell occupied most of the size of the captured image. After sample focusing and cell identification a video was acquired at 100 fps (frames per second) for 1 min, recording the movement of the cell.

As previously mentioned after constructing the new image following the computation of Eq. (1) done per each pixel, the criteria for identification of sub cellular activity can be related to the detection of a change of more than 10 in the values of internal dark pixels of the inspected cells. According to this understanding, the image obtained by taking the temporal STD on a video sequence [31] will be bright in active (changing) zones and dark in quiet areas. The de-facto processing that was applied on the video sequence was as follows: First we performed reducing of the video sequence to a single image containing the standard deviation according to Eq. (1). The gray-level histogram was calculated. Then, a threshold according to the Otsu's method was applied [33]. Otsu's method is used to automatically perform clustering-based image thresholding or, the reduction of a gray level image to a binary image. The algorithm assumes that the image contains two classes of pixels following bi-modal histogram (foreground pixels and background pixels), it then calculates the optimum threshold separating the two classes so that their combined spread (intra-class variance) is minimal. In our case the two classes of pixels are those with strong movements and higher STD and those with softer movements that can be considered inherent to the cell activity and are seen as a dark-gray background in the STD image. Thus in our case as well the aim of the method is to calculate the best threshold so that the combined spread of the two new histogram areas is minimal. In Fig. 1 we demonstrate our algorithm on real RBC images taken as part of our experiment. Fig. 1(a) shows the binary threshold results for healthy cells. As can be seen from the figure, the region inside the rings is empty. For infected cells (trophozoite) an inner region can be seen in white in Fig. 1(b). According to this, classification was done according to the area in white, obtained just counting the number of white pixels, and establishing three reference values. In Fig. 1(c) we show one of the cases where classification failed. Please note that although in the results we present images, all the information used for our processing was taken from experimentally recorded movies that recorded the dynamic behavior of the RBC cells. Thus, our analysis takes the dynamics of the cells into account.

3. Results

To test the performance of our method we prepared two types of RBC cultures: healthy and *P.f* infected. Using a synchronized protocol we could prepare samples with a control parasitemia and in a defined stage (ring, trophozoite) of the parasite cycle inside the cell. Both parasitemia and the stage cycle were confirmed by Giemsa test. The experiments were performed with cultures at two different temperatures of 37 °C and 41 °C to mimic the practical situations of a physiological body temperature and with malaria fever (indeed 41º is a temperature that is specific to malaria but we talk about malaria fever and there 38–40º is the specific range for the bacteria or the virus). For the analysis of the results being presented in this paper, we considered the following:

1. 30 RBCs from healthy culture (20 at 37 °C, 10 at 41 °C)
2. 77 RBCs from infected cultures, as follows
   a. 22 RBCs ring (8 at 37 °C, 14 at 41 °C)
   b. 32 RBCs thropozoite (15 at 37 °C, 17 at 41 °C)
   c. 10 RBCs throphozoite stage, not clearly identified as throphozoite (6 at 37 °C, 4 at 41 °C)
   d. 13 RBCs uninfected (6 at 37 °C, 7 at 41 °C)

Processing the healthy cell videos with the voxel algorithm described in Section 2.2 produces the final images which allow classification of the cell in infected or uninfected. The results obtained processing all the 30 cells from healthy cultures are shown in Table 1. In this table we have three lines. The first relates to cells at temperature of 37 °C. There we inspected 20 cells and properly identified 18 out of them. The second line relates to cells at temperature of 41 °C. There we inspected 10 healthy cells and correctly identified all of them. The third line is the summary of the results presented in the first two lines. Thus, the cells are correctly classified as healthy cells in 28/30 cases 18/20 cases for 37 °C and 10/10 for 41 °C.

We repeated the approach for the videos recorded for RBCs coming from infected cultures. The results for the RBCs coming from infected cultures are shown in Table 2. The table is divided into several sections presenting the results of the proposed approach for analyzing rings, trophozoites, other types of cells (from infected trophozoite stage but throphozoite not clearly identified) and uninfected cells (does not mean they are healthy). In all of those four categories we had cells at temperature of 37 °C and 41 °C. As in Table 1 the middle row shows how many out of the inspected cells in each category were correctly identified and the third row (from left) computes the identification statistics in %. The cells are correctly classified in 71/77 situations. Detection of infected RBCs (61/64) seems better than detection of uninfected cells (10/13). The results show a very good detection for the throphozoite (32/32) for both temperatures, good detection for
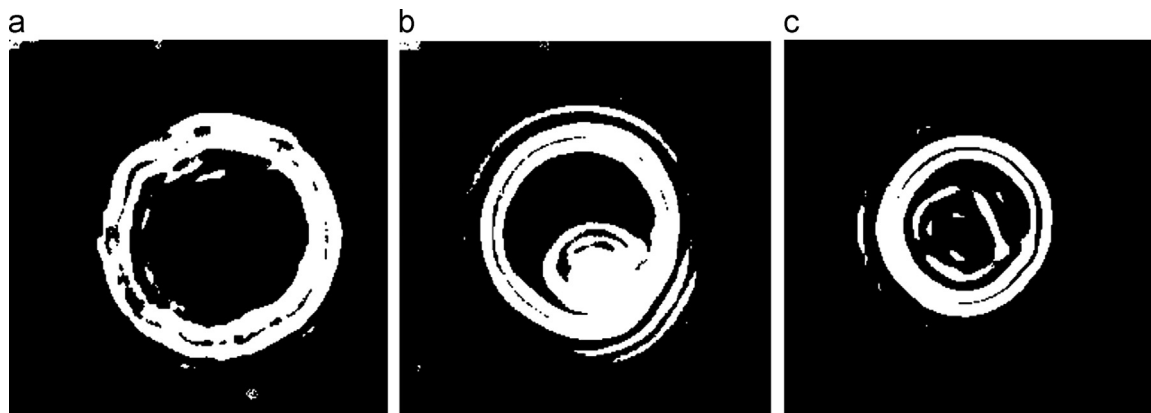

Fig. 1. Demonstration of the proposed algorithm on experimentally captured images. The binary threshold results for: (a) Healthy cells. (b) Infected cells (trophozoite). (c) One example case where classification failed.

Table 1
Correctly identified cells. RBC in healthy culture – 30 cells analyzed.

Healthy culture	Identified/total	%
37 °C	18/20	90
41 °C	10/10	100
Total healthy (37 °C+41 °C)	**28/30**	**93.3**

Table 2
Results from infected cultures. RBC in *P.f* culture – 67 cells analyzed.

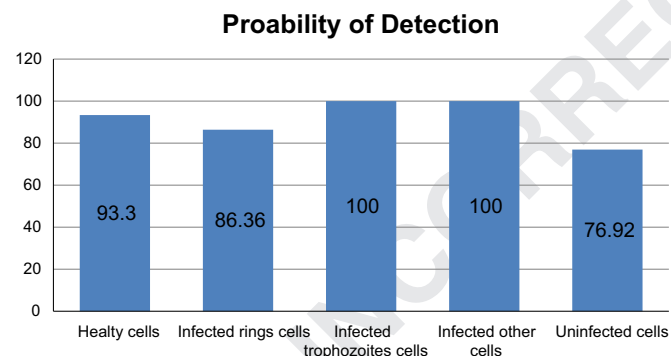| P.f culture	Identified/total	%
Rings		
37 °C	7/8	87.5
41 °C	12/14	85.71
Total rings (37 °C+ 41 °C)	**19/22**	**86.36**
Trophozoites		
37 °C	15/15	100
41 °C	17/17	100
Total trophozoites (37 °C+41 °C)	**32/32**	**100**
Other (from infected trophozoite stage but throphozoite not clearly identified)		
37 °C	6/6	100
41 °C	4/4	100
Total other (37 °C+ 41 °C)	**10/10**	**100**
Uninfected		
37 °C	4/6	66.67
41 °C	6/7	85.71
Total uninfected (37 °C+41 °C)	**10/13**	**76.92**

Fig. 2. Graphical visualization of the detection probability as it is presented in Tables 1 and 2.

rings (19/22) for both temperatures, and relatively good detection for uninfected cells (10/13) with lower rate for 37 °C (4/6). Moreover we considered also cells (N=10) from throphozoite stage but for which the throphozoite could not be clearly identified from the video. The appearance of the cells presents conformations like knobs but since *P.f* (W2 strain) culture was used, the presence of the knobs should be excluded. However, also in this case detection as infected is very good (10/10). For visualization purposes in Fig. 2 we summarize the detection results presented in Tables 1 and 2.

Please note that the cells analyzed in this paper were analyzed in parallel by an expert of malaria who manually checked and characterized them while in parallel they were inspected by our automated image processing algorithm. So the setting of the reference status of the cells to which the outcome of our algorithm was compared was done by a malaria expert who has collected the samples.

Examples of final images resulting for each type of category of cells (appearing in Tables 1 and 2) are presented in Fig. 3. In the

Fig. 3 we show the experimentally acquired cells for each one of the 5 categories (healthy, rings, trophoziotes, others and uninfected) for the reader to better visualize how the images that our algorithm processed look like. We also showed in the case of rings and uninfected cells example image of cells that were not properly recognized by our algorithm.

After computing the overall hit and miss probabilities for infected as well as for the uninfected RBC we get that for infected cells the miss probability is around 5% and the hit probability is above 95%. For the case of uninfected cells the miss probability is below 12% and the hit probability is above 88%.

4. Discussions

In this paper we have presented a new voxel based algorithm for detecting of malaria at its different stages of development.

The image processing algorithm that we have developed aims to localize the movement of the RBC and to detect whether it has some spatial dependence. We have analyzed more than 100 RBCs (30 from healthy and 77 from infected cultures) using the voxel algorithm to detect infected and uninfected RBCs from healthy and *P.f.* infected cultures. As shown in the Results section, the detection of infected cells is very good and it is above 95% (false negative probability of less than 5%) while the detection of uninfected cells (RBCs from healthy culture are included here) is less precise and it is around 88.4% (false positive probability of less than 12%). It is important to note that it is much more critical to have very low false negative probability rather than false positive. The number of samples is still low to be statistically relevant and more data should be collected and analyzed in the future. However, we consider as positive the fact that the detection of infected cells has a higher rate of success than the detection of uninfected cells. If so called false negatives (uninfected cells classified as infected) are detected, this calls for an alternative analysis of the sample or repetition of data collection and analysis which is however less dangerous than missing false positives (infected cells classified as uninfected).

More than 100 images of RBC were inspected and analyzed using the proposed algorithm. Based on the outcome of the composed approach we demonstrated the possibility of being able to distinguish between the different stages/phases of malaria starting from the ring stage parasites, early trophozoites and up to late stage schizonts. Based on the available samples we had, the analysis was indeed performed on RBC at different stages of infection.

Regarding the developed algorithm, the basic problem with our method is that, strictly speaking, the Otsu's method applies on bimodal histograms and most of our images are almost monomodal with a clear dominance of the darker parts. Additionally, results were quite close to those obtained by simple visual inspection that was much faster. Visual classification form of the STD image was found to be easy and intuitive. Therefore, we decided to leave only the first part of the image processing which includes making the visual classification.

Regarding the processing time of the proposed algorithm, it was in the order of milli seconds but part of the processing was done using Matlab program and real time programing can significantly reduce the processing time. Although the computational complexity is in the order of N, where N is the number of pixels, in order to reach a decision only a portion of the pixels of the image should be analyzed.

5. Conclusions

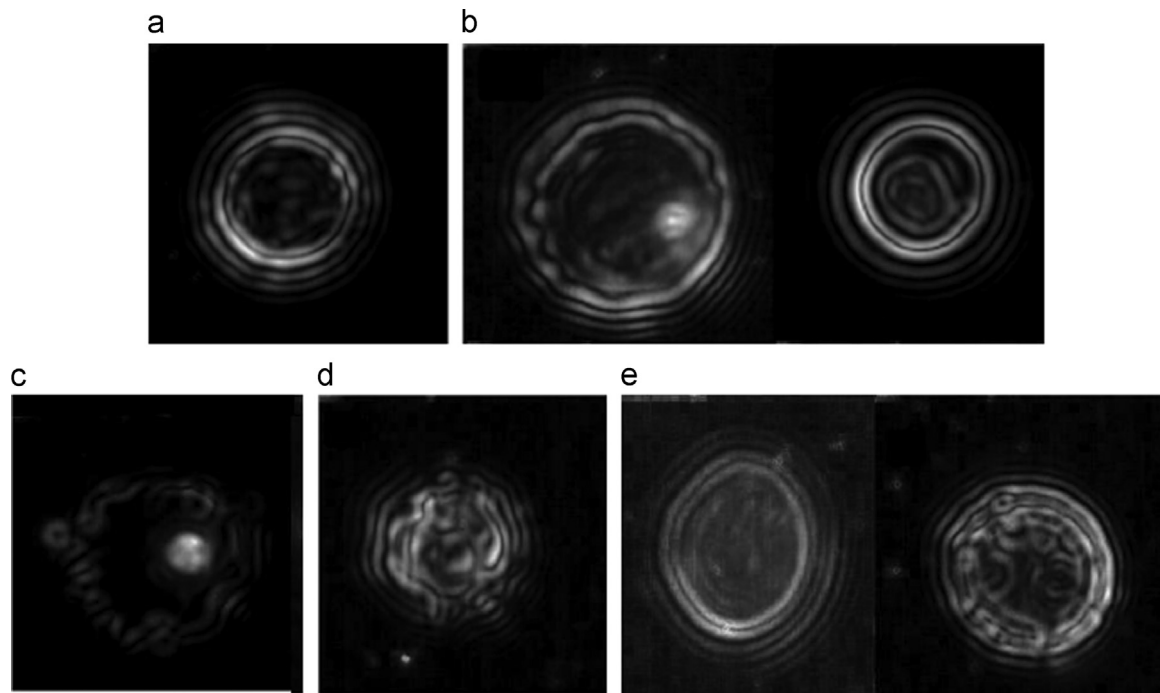In this paper we have developed and experimentally validated

Fig. 3. Example of the experimentally acquired cells images that were analyzed by the proposed algorithm. The cells presented are the representing example of RBCs from each one of the 5 categories of cells that were analyzed in our experiment: (a) Healthy, properly identified cell. (b) Rings. On the left properly identified and on the right wrongly identified. (c) Throphozoites, properly identified. (d) Other cells, properly identified. (e) Uninfected. On the left properly identified and on the right wrongly identified.

a novel image processing algorithm associated with microscopy hardware capable of performing real time detection of malaria infection. The proposed algorithm analyzes the local movements within the red blood cell and its validation showed that it could detect infected cells with probability above 93% while healthy cells with probability of above 85%. The numerical tools used for our analysis are freely available to the community thus being accessible in endemic countries and areas with limited incomes.

It is important to emphasize that the concept presented in our paper is preliminary and still a significant amount of experimental work should be done in order to fully validate the proposed concept as an efficient approach for malaria detection. It is important to note that the results we have obtained in this paper only intend to demonstrate the preliminary potential that our technique has in inspection of RBC images.

References

[1] WHO (Ed.), World Malaria Report 2013 in WHO Library Cataloguing in Publication Data, ⟨http://www.who.int/malaria/publications/world_malaria_report_2013/en/⟩.

[2] C.K. Murray, R.A. Gasser Jr., A.J. Magill, R.S. Miller, Update on rapid diagnostic testing for malaria, Clin. Microbiol. Rev. 21 (1) (2008) 97–110.

[3] C. Wongsrichanalai, M.J. Barcus, S. Muth, A. Sutamihardja, W.H. Wernsdorfer, A review of malaria diagnostic tools: microscopy and rapid diagnostic test (RDT), Am. J. Trop. Med. Hyg. 77 (6 Suppl) (2007) 119–127.

[4] A. Fontaine, S. Bourdon, M. Belghazi, M. Pophillat, P. Fourquet, S. Granjeaud, M. Torrentino-Madamet, C. Rogier, T. Fusai, L. Almeras, Plasmodium falciparum infection-induced changes in erythrocyte membrane proteins, Parasitol. Res. 110 (2) (2012) 545–556.

[5] J.P. Shelby, J. White, K. Ganesan, P.K. Rathod, D.T. Chiu, A microfluidic model for single-cell capillary obstruction by Plasmodium falciparum-infected erythrocytes, Proc. Natl. Acad. Sci. U.S.A. 100 (25) (2003) 14618–14622.

[6] J.P. Mills, M. Diez-Silva, D.J. Quinn, M. Dao, M.J. Lang, K.S.W. Tan, C.T. Lim, G. Milon, P.H. David, O. Mercereau-Puijalon, S. Bonnefoy, S. Suresh, Effect of plasmodial RESA protein on deformability of human red blood cells harboring Plasmodium falciparum, Proc. Natl. Acad. Sci. U.S.A. 104 (22) (2007) 9213–9217.

[7] F. Omodeo-Salè, A. Motti, N. Basilico, S. Parapini, P. Olliaro, D. Taramelli, Accelerated senescence of human erythrocytes cultured with Plasmodium falciparum, Blood 102 (2) (2003) 705–711.

[8] F. Omodeo-Salè, A. Motti, A. Dondorp, N.J. White, D. Taramelli, Destabilisation and subsequent lysis of human erythrocytes induced by Plasmodium falciparum haem products, Eur. J. Haematol. 74 (4) (2005) 324–332.

[9] C.A. Moxon, G.E. Grau, A.G. Craig, Malaria: modification of the red blood cell and consequences in the human host, Br. J. Haematol. 154 (2011) 670–679.

[10] S. Suresh, J. Spatz, J.P. Mills, A. Micoulet, M. Dao, C.T. Lim, M. Beil, T. Seufferlein, Connections between single-cell biomechanics and human disease states: gastrointestinal cancer and malaria, Acta Biomater. 1 (1) (2005) 15–30.

[11] L. Gervais, N. de Rooij, E. Delamarche, Microfluidic chips for point-of-care immunodiagnostics, Adv. Mater. 23 (24) (2011) H151–H176.

[12] R. Fan, O. Vermesh, A. Srivastava, B.K.H. Yen, L. Qin, H. Ahmad, G.A. Kwong, C.-C. Liu, J. Gould, L. Hood, J.R. Heath, Integrated barcode chips for rapid, multiplexed analysis of proteins in microliter quantities of blood, Nat. Biotechnol. 26 (12) (2008) 1373–1378.

[13] R. Lima, T. Ishikawa, Y. Imai, M. Takeda, S. Wada, T. Yamaguchi, Radial dispersion of red blood cells in blood flowing through glass capillaries: the role of hematocrit and geometry, J. Biomech. 41 (10) (2008) 2188–2196.

[14] H.W. Hou, A.A.S. Bhagat, A.G.L. Chong, P. Mao, K.S.W. Tan, J. Han, C.T. Lim, Deformability based cell margination–a simple microfluidic design for malaria-infected erythrocyte separation, Lab Chip 10 (19) (2010) 2605–2613.

[15] H. Bow, I.V. Pivkin, M. Diez-Silva, S.J. Goldfless, M. Dao, J.C. Niles, S. Suresh, J. Han, A microfabricated deformability-based flow cytometer with application to malaria, Lab Chip 11 (6) (2011) 1065–1073.

[16] E.N. Strohm, E. Hysi, M.C. Kolios, Photoacoustic measurements of single red blood cells, in: Proceeding of the IEEE International Ultrasonics Symposium (IUS), 2013, pp. 1406–1409.

[17] M.L. Li, P.H. Wang, Optical resolution photoacoustic microscopy using a Blu-ray DVD pickup head, in: Proceedings of the SPIE Conference on Photons Plus Ultrasound: Imaging and Sensing, Vol. 8943, 2014, 894315, doi: 10.1117/12.2037146.March 3.

[18] V.P. Zharov, E.I. Galanzha, E.V. Shashkov, N.G. Khlebtsov, V.V. Tuchin, In vivo photoacoustic flow cytometry for monitoring of circulating single cancer cells and contrast agents, Opt. Lett. 31 (2006) 3623–3625.

[19] G. Popescu, T. Ikeda, R.R. Dasari, M.S. Feld, Diffraction phase microscopy for quantifying cell structure and dynamics, Opt. Lett. 31 (6) (2006) 775–777.

[20] G. Popescu, Y. Park, W. Choi, R.R. Dasari, M.S. Feld, K. Badizadegan, Imaging red blood cell dynamics by quantitative phase microscopy, Blood Cells Mol. Dis. 41 (1) (2008) 10–16.

[21] D. Cojoc, S. Finaurini, P. Livshits, E. Gur, A. Shapira, V. Mico, Z. Zalevsky, Toward fast malaria detection by secondary speckle sensing microscopy, Biomed. Opt. Express 3 (2012) 991–1005.

[22] I. Moon, A. Anand, M. Cruz, B. Javidi, Identification of malaria-infected red blood cells via digital shearing interferometry and statistical inference, IEEE Photonics J. 5 (2013) 6900207.

[23] G. Popescu, Y.K. Park, K. Badizadegan, R.R. Dasari, M.S. Feld, Diffraction phase and fluorescence microscopy, Opt. Express 14 (18) (2006) 8263–8268.

[24] Y. Park, M. Diez-Silva, G. Popescu, G. Lykotrafitis, W. Choi, M.S. Feld, S. Suresh, Refractive index maps and membrane dynamics of human red blood cells parasitized by Plasmodium falciparum, Proc. Natl. Acad. Sci. U.S.A. 105 (2008) 13730–13735.

[25] C.S. Yelleswarapu, M. Tipping, S.R. Kothapalli, A. Veraksa, D.V. Rao, Common-path multimodal optical microscopy, Opt. Lett. 34 (8) (2009) 1243–1245.

[26] N. Pavillon, A. Benke, D. Boss, C. Moratal, J. Kühn, P. Jourdain, C. Depeursinge, P. J. Magistretti, P. Marquet, Cell morphology and intracellular ionic homeostasis explored with a multimodal approach combining epifluorescence and digital holographic microscopy, J. Biophotonics 3 (7) (2010) 432–436.

[27] Y. Park, M. Diez-Silva, D. Fu, G. Popescu, W. Choi, I. Barman, S. Suresh, M. S. Feld, Static and dynamic light scattering of healthy and malaria-parasite invaded red blood cell, J. Biomed. Opt. 15 (2) (2010) 020506.

[28] P. Memmolo, L. Miccio, F. Merola, O. Gennari, P. Antonio Netti1,3, P. Ferraro, 3D morphometry of red blood cells by digital holography, Cytometry 85 (2014) 1030–1036.

[29] K. Kim, Z. Yaqoob, K. Lee, J. Woong Kang, Y. Choi, P. Hosseini, P.T.C. So, Y. Park, Diffraction optical tomography using a quantitative phase imaging unit, Opt. Lett. 39 (2014) 6935–6938.

[30] T. Kim, R. Zhou, M. Mir, S.D. Babacan, P.S. Carney, L.L. Goddard, G. Popescu, White-light diffraction tomography of unlabelled live cells, Nat. Photonics 8 (2014) 256–263.

[31] ImageJ:Image Processing and Analysis in Java at: ⟨http://imagej.nih.gov/ij/⟩ and relevant plugin at: ⟨http://rsb.info.nih.gov/ij/macros/tools/VideoCapture Tool.txt⟩.

[32] W. Trager, J.B. Jensen, Human malaria parasites in continuous culture, Science 193 (4254) (1976) 673–675.

[33] M. Sezgin, B. Sankur, Survey over image thresholding techniques and quantitative performance evaluation, J. Electron. Imaging 13 (1) (2004) 146–165.